



## **Elevated temperature fatigue S-N curve behavior for three different carbon percentage steel alloys**

**Hussain J. Mohammed Al-Alkawi<sup>1</sup>, Mohammed H. Ali<sup>2</sup>, Shaimaa Ghazy Mezban<sup>2</sup>**

<sup>1</sup> University of Technology, Electromechanical Engineering Department, Baghdad, Iraq.

<sup>2</sup> University of Al-Mustansiriya, Collage of Engineering, Material Engineering Department, Baghdad, Iraq.

Received 5 Aug. 2016; Received in revised form 28 Aug. 2016; Accepted 31 Aug. 2016; Available online 1 July 2017

### **Abstract**

Constant Fatigue life analysis was done to predict the fatigue life of carbon steel alloy specimens with three different content of carbon (0.758%C, 0.539%C and 0.319%C) under effect of temperature. The fatigue experiments were performed at room temperature (RT) and 100°C with the frequency of 23.34 Hz on a cantilever rotating bending fatigue testing machine. Constant amplitude fatigue test results at room temperature were compared with the fatigue test results at high temperature. The results showed that the fatigue life and fatigue strength decrease at elevated temperature (100°C) as compared to room temperature. Carbon content also had a great effect on fatigue properties in which increasing carbon percentage led to improve the fatigue strength and life up to 0.539%C, but fatigue properties decreased when carbon content exceeded that value.

**Copyright © 2017 International Energy and Environment Foundation - All rights reserved.**

**Keywords:** Thermal constant fatigue testing; Different carbon percentage; Carbon steel alloys.

### **1. Introduction**

The use of carbon steel in the industry is because of its cost, ease of fabrication, weld-ability, availability, and so on. Carbon steel is used in moderate temperature service systems such as boilers, piping and heat exchangers where good strength and ductility is desired. The most important alloying element in carbon steel is carbon because small variations in the level of carbon in the composition will cause significant differences in properties like hardness, strength and ductility [1]. For example, tensile strength, wear resistance and surface hardening increase with increasing carbon content and weld-ability decreases [2]. In 1850, it was found that when a material is subjected to cyclic loading, it would fail due to the application of stresses that are much lower than that is subjected to static loading. Failures occurring under dynamic loading conditions are called fatigue failures and these failures occur after a considerable period of service [3]. Fatigue can occur by the formation of a small crack, the crack then propagates slowly through the material in a direction perpendicular to the main tensile axis. Automobiles, aircraft wings, ships, jet engines and turbines are all subjected to fatigue failures [4]. Metallic materials that are subjected to cyclic loading at high temperature will be damaged in a complex manner which can be hardly described. When a component is exposed to thermo-mechanical fatigue (TMF) loading conditions, a combination of thermal transients with mechanical strain cycles will result during startup and shut down of the component. The extent of this damage depends strongly on the specific material

and the loading conditions applied [5]. Damage of the component is affected by the change in the rate of temperature. So, severe temperature changes may result in formation of plastic deformation in surface layers in the presence or absence of mechanical loading which in turn can lead to initiation of cracks [6]. The present work aims to study the effect of high temperature 100°C on the fatigue properties of three different carbon steel alloys and compare the results with the (RT) behavior.

## 2. Literature survey

Jong I. Park et.al [7]; examined the thermal fatigue life of five different high speed steel (HSS) rolls with different chemical composition. The basic microstructures were formed mainly of coarse primary carbides and tempered martensite matrix. Due to thermal fatigue, the cracks were begun on primary carbides located on surface of the specimen and propagated along the primary carbides. The experimental results showed that the thermal fatigue life of each roll decreases with increasing the temperature. It was found that to improve the thermal fatigue property of HSS rolls; roll materials should have a fine and uniform distribution of primary carbides in order to lower the fatigue crack initiation sites. S. A. Agbadua et.al [8]; examined the effect of thermal cycling on fatigue behavior of Fe-0.2045C low carbon steel. The specimens were exposed to four different cycling temperatures: 120°C, 220°C, 360°C and 500°C. It was shown that low carbon steel has good fatigue resistance between 120-220°C as a result of low carbide proportion and little inclusions. At 360°C, the low carbon steel has the lowest fatigue strength as a result of increased proportion of inclusions or impurities such as oxides and sulfides. At a temperature of 500°C, it has a better fatigue resistance then at 360°C. It was concluded that low carbon steel has fatigue limit between 20°C-220°C. Qasim Bader and Emad Kadum [9]; studied the fatigue life estimation of carbon steel alloy specimens with different carbon content at room temperature. The fatigue tests were carried out applying a fully reversed cyclic load with the frequency of 50 Hz on a cantilever rotating bending fatigue testing machine. It was observed that fatigue limit increase with increasing hardness and carbon content. P. Gallo and F. Berto [10]; investigated the high temperature fatigue on fatigue strength of 40CrMoV13.9 steel. The test was conducted at different temperatures up to 650°C. The results showed that 40CrMoV13.9 steel exhibits good fatigue behavior up to 500°C and until that temperature, no reduction in fatigue strength was observed with respect to room temperature. But above 500°C, a significant reduction in fatigue strength was detected

## 3. Experimental work

The material used in this study was carbon steel in the form of round solid bar with three different carbon contents: 0.758%C, 0.539%C and 0.319%C. The chemical analysis was carried out at (State Company for Inspection and Engineering Rehabilitation (SIER) in Iraq). The chemical compositions of each group are given in Table 1.

Table 1. Chemical composition of three groups of carbon steel.

| Group   | Standard ASTM A 29/A 29M-05 [11]  |           |        |       |       |       |        |       |
|---------|-----------------------------------|-----------|--------|-------|-------|-------|--------|-------|
|         | C%                                | Mn        | P      | S     | Cr    | Ni    | Al     | Cu    |
| (A)1075 | 0.70-0.80                         | 0.40-0.70 | 0.04   | 0.05  | 0.158 | 0.059 | 0.034  | 0.043 |
| (B)1053 | 0.48-0.55                         | 0.70-1.00 | 0.04   | 0.05  | 0.66  | 1.7   | 0.033  | 0.116 |
| (C)1030 | 0.28-0.34                         | 0.60-0.90 | 0.04   | 0.05  | 0.90  | 0.08  | 0.0048 | 0.091 |
| Group   | Experimental Chemical Composition |           |        |       |       |       |        |       |
|         | C%                                | Mn        | P      | S     | Cr    | Ni    | Al     | Cu    |
| A       | 0.758                             | 0.297     | 0.0006 | 0.006 | 0.160 | 0.066 | 0.035  | 0.044 |
| B       | 0.539                             | 0.623     | 0.006  | 0.001 | 0.730 | 1.67  | 0.032  | 0.115 |
| C       | 0.319                             | 0.607     | 0.002  | 0.001 | 0.911 | 0.081 | 0.005  | 0.092 |

Tensile test was conducted at room temperature to obtain mechanical properties such as ultimate strength, yield strength, percentage of elongation and modulus of elasticity. All mechanical tests were done at the University Of Technology, Materials Department. The tensile test rig used is WDW-50 illustrated in Figure 1 and the mechanical properties obtained from the tests are shown in Table 2. The shape and dimensions of tensile specimen was selected according to ASTM (A370-11) standard specification.

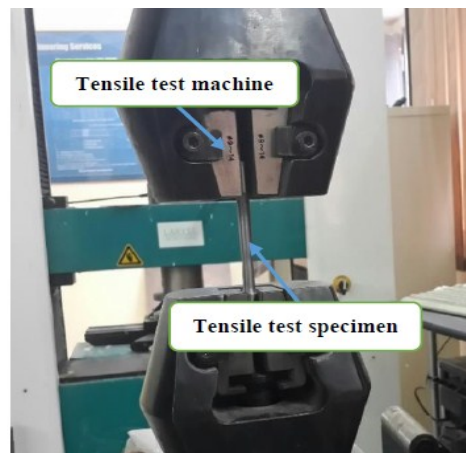


Figure 1. Tensile test machine type Laryee WDW-50.

Table 2. Mechanical properties of carbon steel alloy (Results of average three specimens).

| Group | C%    | Ultimate Stress<br>$\sigma_u$ , [MPa] | Yield stress $\sigma_y$ ,<br>[MPa] | Elongation<br>[%] | Modulus of<br>elasticity E, [GPa] |
|-------|-------|---------------------------------------|------------------------------------|-------------------|-----------------------------------|
| 1075  | 0.758 | 820                                   | 480                                | 26.5              | 205                               |
| 1053  | 0.539 | 691                                   | 377                                | 38.4              | 204                               |
| 1030  | 0.319 | 804                                   | 462                                | 27.79             | 207                               |

#### 4. Fatigue testing

All fatigue tests were done using fatigue testing machine Schenck product of type PUNN rotating bending as shown in Figure 2. The test was done at University of Technology, electromechanical engineering department. In the fatigue testing machine, a rotating sample which is clamped on both sides is loaded and rotated about its own axis with the help of a motor. Following a certain number of load cycles, the specimen will rupture as a result of material fatigue. The number of cycles to failure was recorded using a counter. All fatigue tests were performed at 1400 rpm (23.34 Hz).

To carry out any fatigue experiment, a consistent set of specimens must be prepared. The standard fatigue specimens were prepared according to DIN 50113 standard specification as shown in Figure 3.

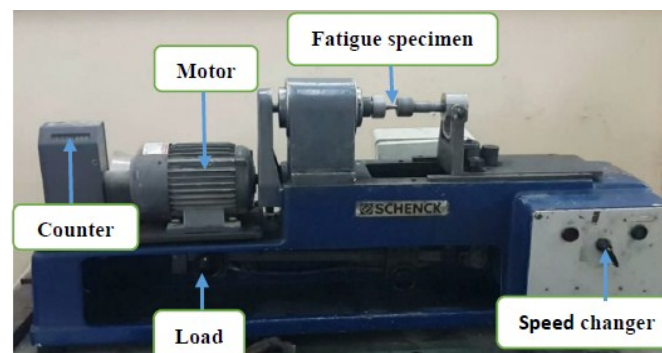


Figure 2. PUNN rotating fatigue bending machine.

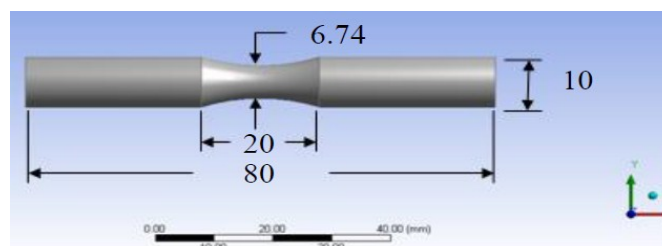


Figure 3. Fatigue test specimen dimensions in millimeter according to (DIN 50113) standard specification.

## 5. Thermal fatigue test

For the thermal fatigue test, thermal loading tests were conducted using a small furnace. The furnace is used to heat the environment of the specimens to the required temperature. Figure 4 shows the furnace attached to the fatigue testing machine with a digital thermal control unit board. A K-type thermocouple is necessary to be used to control the heating temperature inside the furnace.

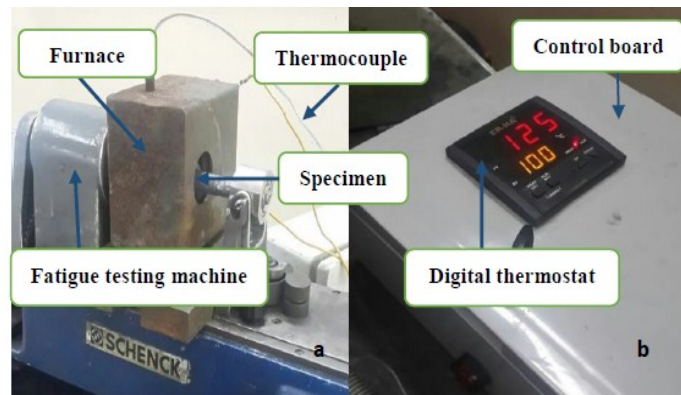


Figure 4. (a) Furnace attached to fatigue machine, (b) digital thermal electrical control unit board.

## 6. Experimental results and discussion

### 6.1 Room temperature fatigue test results

The first series of the fatigue testing was carried out at room temperature (RT) using the three carbon steel alloys in order to obtain S-N curve behavior for each alloy of carbon mentioned in Table 1. The constant applied stresses used for each carbon percentage were 500MPa, 400MPa, 300MPa and 200MPa and three specimens were tested at each stress level. The number of cycles to failure was recorded using a counter and the applied stress remained constant without changing until the fatigue failure occurred. Table 3 shows fatigue test results at room temperature.

Table 3. Fatigue test results at room temperature.

| Specimen No.            | Applied Stress [MPa] | $N_f$ Cycles         | $N_{f, average}$ |
|-------------------------|----------------------|----------------------|------------------|
| Group A (0.758% Carbon) |                      |                      |                  |
| 1,2,3                   | 500                  | 2000,3000,1300       | 2100             |
| 4,5,6                   | 400                  | 11000, 9500,12500    | 11000            |
| 7,8,9                   | 300                  | 52000,62000,44000    | 52666            |
| 10,11,12                | 200                  | 395000,410000,366000 | 390333           |
| Group B (0.539% Carbon) |                      |                      |                  |
| 13,14,15                | 500                  | 1200,2000,3000       | 2066             |
| 16,17,18                | 400                  | 7000,10000,11000     | 9333             |
| 19,20,21                | 300                  | 116000,122000,130000 | 122666           |
| 22,23,24                | 200                  | 420000,380000,460000 | 420000           |
| Group C (0.319% Carbon) |                      |                      |                  |
| 25,26,27                | 500                  | 10000,12000,14000    | 12000            |
| 28,29,30                | 400                  | 19000,22000,26000    | 22333            |
| 31,32,33                | 300                  | 140000,125000,110000 | 125000           |
| 34,35,36                | 200                  | 320000,290000,370000 | 326666           |

The typical trend of fatigue tests data plotted by the relationship between applied stress and number of cycles can be expressed in power law regression (Basquin equation) as the following equation [12].

$$\sigma_f = \sigma'_f N_f^\alpha \quad (1)$$

where  $\sigma_f$  is the applied stress sometime defined by stress at failure for constant amplitude tests.  $\sigma_f$  is related to static bending strength, while the coefficient ( $\alpha$ ) is related to the fatigue degradation and describes the fatigue sensitivity.

The above data are plotted according to Basquin equation in Figure 5 which shows the behavior of the three carbon content alloys at room temperature.

A correlation factor ( $R^2$ ) was used to verify whether the experimental results are well described by power formula. The value of  $R^2$  can be calculated by equations mentioned in Ref [13]. The closer is  $R^2$  to unity; the stronger is the relationship between stress ( $\sigma_f$ ) and average cycles ( $N_{fav}$ ).

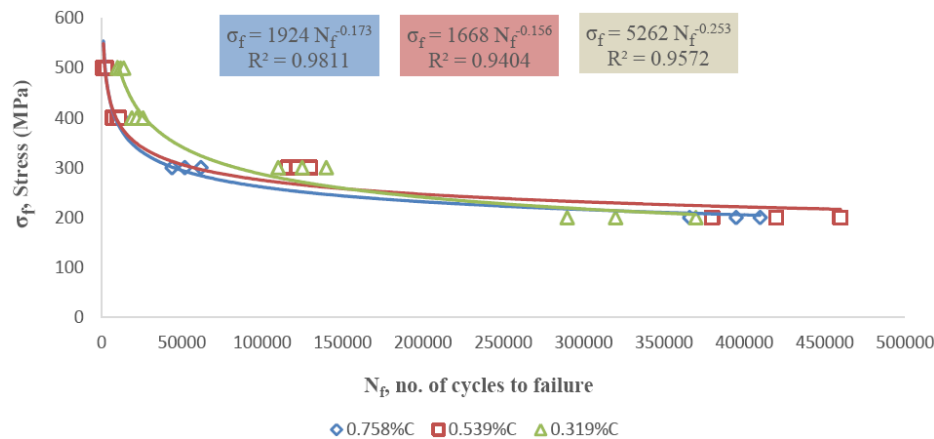


Figure 5. S-N curves for three carbon steel alloys at room temperature.

### 6.2 Fatigue test results at 100°C

The fatigue test was done at constant load and constant temperature. The temperature used was at 100°C and remained constant until failure of the specimen occurred. The stresses used for each group of carbon content were 500MPa, 400MPa, 300MPa and 200MPa and three tests were performed at each stress level. Table 4 gives the results of the fatigue tests at 100°C for the three carbon steel alloys and Figure 6 shows the behavior of the three carbon content alloys at 100°C. Table 5 shows a comparison between the behavior of the three alloys at (RT) and 100°C.

The fatigue limits at  $10^7$  cycles were determined for the three alloys corresponding to carbon content percentage for both cases (RT and 100°C) are given in Table 6.

Figure 7 shows the variation of fatigue limit of the three alloys related to the carbon percentage at room temperature and 100°C. The fatigue limits for the three alloys reduced due to 100°C environment. The high reduction was occurred for 0.758%C as shown in Figure 8.

Table 4. Constant fatigue test results at 100°C.

| Specimen No.            | Applied Stress [MPa] | $N_f$ Cycles         | $N_{f, average}$ |
|-------------------------|----------------------|----------------------|------------------|
| Group A (0.758% Carbon) |                      |                      |                  |
| 37,38,39                | 500                  | 1000,1500,2000       | 1500             |
| 40,41,42                | 400                  | 8000,7000,5000       | 6666             |
| 43,44,45                | 300                  | 31000,28000,22000    | 27000            |
| 46,47,48                | 200                  | 115000,144000,166000 | 141666           |
| Group B (0.539% Carbon) |                      |                      |                  |
| 49,50,51                | 500                  | 1000,2000,1000       | 1333             |
| 52,53,54                | 400                  | 3000,7000,9000       | 6333             |
| 55,56,57                | 300                  | 90000,82000,75000    | 82333            |
| 58,59,60                | 200                  | 120000,126000,98000  | 114666           |
| Group C (0.319% Carbon) |                      |                      |                  |
| 61,62,63                | 500                  | 6000,4000,8000       | 6000             |
| 64,65,66                | 400                  | 12000,16000,20000    | 16000            |
| 67,68,69                | 300                  | 88000,72000,60000    | 73333            |
| 70,71,72                | 200                  | 100000,121000,135000 | 118666           |

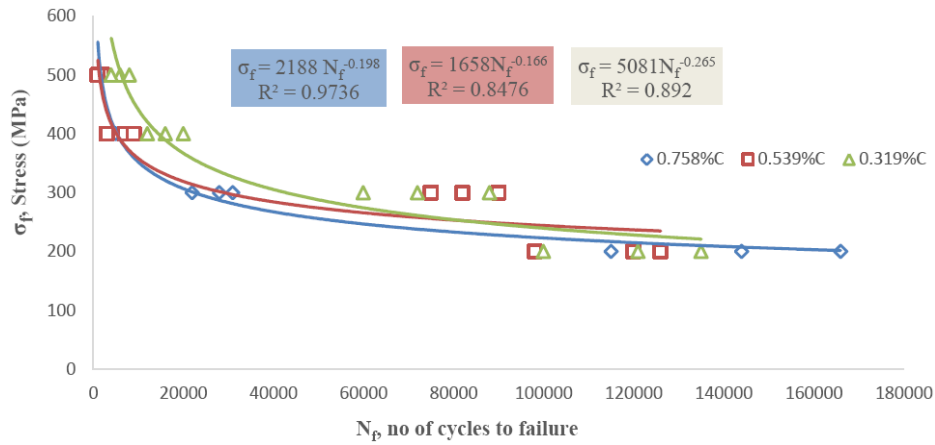


Figure 6. S-N curves for three alloys at 100°C.

Table 5. S-N curves equations at room temperature (25°C) and 100°C.

| Room temperature (25°C)        | 100°C                          |
|--------------------------------|--------------------------------|
| 0.758%C                        |                                |
| $\sigma_f = 1924 N_f^{-0.173}$ | $\sigma_f = 2188 N_f^{-0.198}$ |
| 0.539%C                        |                                |
| $\sigma_f = 1668 N_f^{-0.156}$ | $\sigma_f = 1658 N_f^{-0.166}$ |
| 0.319%C                        |                                |
| $\sigma_f = 5262 N_f^{-0.253}$ | $\sigma_f = 5081 N_f^{-0.265}$ |

Table 6. Fatigue limits reduction percentage due to 100°C.

| 0.758%C  | 0.539%C | 0.319%C |
|--|---------|---------|
| Fatigue limits [MPa] at RT                           |         |         |
| 118.36   | 134.95  | 89.15   |
| Fatigue limits [MPa] at 100°C                        |         |         |
| 89.95  | 114.17  | 70.94   |
| Reduction in fatigue limits [%] at 100°C environment |         |         |
| 24%  | 15.39%  | 20.42%  |

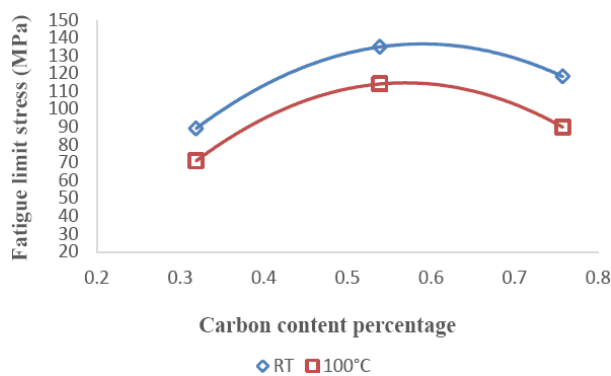


Figure 7. Variation of fatigue limit at RT and 100°C.

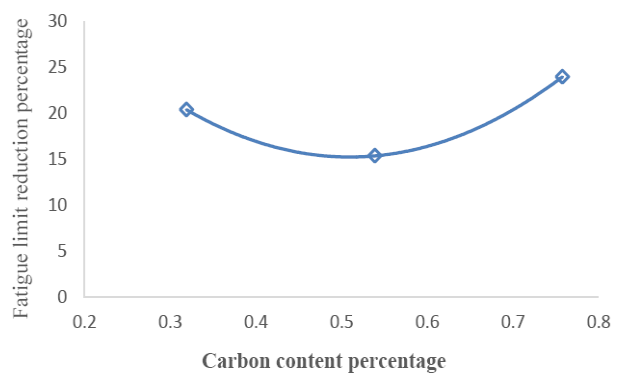


Figure 8. Reduction of fatigue limit for three carbon steel alloys.

It is clear that the worst case was happened in 0.758%C which revealed high reduction in fatigue limit and the best alloy is 0.539%C which gave less reducing in fatigue limit. the above behavior may be due to high strain aging occurred in 0.539%C alloy while a weak strain aging in 0.758%C at 100°C thermal fatigue [14].

### 6.3 Comparison between fatigue life for the three alloys at 100°C

Table 7 shows the comparison of the constant fatigue life of the three alloys mentioned at different stress levels based on the S-N curves equations. It is clear that the high carbon content has high reduction percentage, 24% compared to the alloy of 0.539%C which exhibited 15.39% while the 0.319%C gave 20.42% reduction. The reduction percentage (RP) for the three alloys is calculated using the equation:

$$RP = \frac{(\sigma_{F.L})_{RT} - (\sigma_{F.L})_{100^{\circ}C}}{(\sigma_{F.L})_{RT}} \quad (2)$$

Table 7. Fatigue life predictions at 100°C for three alloys.

| Applied stress [MPa] | Predicted life | Experimental life | $\frac{\text{predicted life}}{\text{experimental life}}$ |
|----------------------|----------------|-------------------|--|
| 0.758%C              |                |                   |  |
| 500                  | 1729           | 1500              | 1.1526   |
| 400                  | 5336           | 6666              | 0.8004   |
| 300                  | 22815          | 27000             | 0.845  |
| 200                  | 176883         | 141666            | 1.2485   |
| 0.539%C              |                |                   |  |
| 500                  | 1368           | 1333              | 1.0262   |
| 400                  | 5248           | 6333              | 0.8286   |
| 300                  | 29694          | 82333             | 0.3606   |
| 200                  | 341555         | 114666            | 2.9786   |
| 0.319%C              |                |                   |  |
| 500                  | 6308           | 6000              | 1.0513   |
| 400                  | 14643          | 16000             | 0.9151   |
| 300                  | 43360          | 73333             | 0.5912   |
| 200                  | 200254         | 118666            | 1.6875   |

Figure 9 reveals that the predicted life is slightly larger than the experimental life for stress levels 500 and 200MPa while at 400 and 300MPa the experimental life is larger than the predicted life for the three alloys. The diagram observes that the estimated fatigue life coincides well with the experimental fatigue life. Alalkawi et.al [15] concluded that the low carbon content percentage show a large degree of cyclic softening and the fatigue life and strength are lower than that of medium and high carbon content percentage. Also they observed that the ratio of predicted to experimental life located around unity (larger than one) for high cycle fatigue while the low cycle fatigue life becomes less than unity.

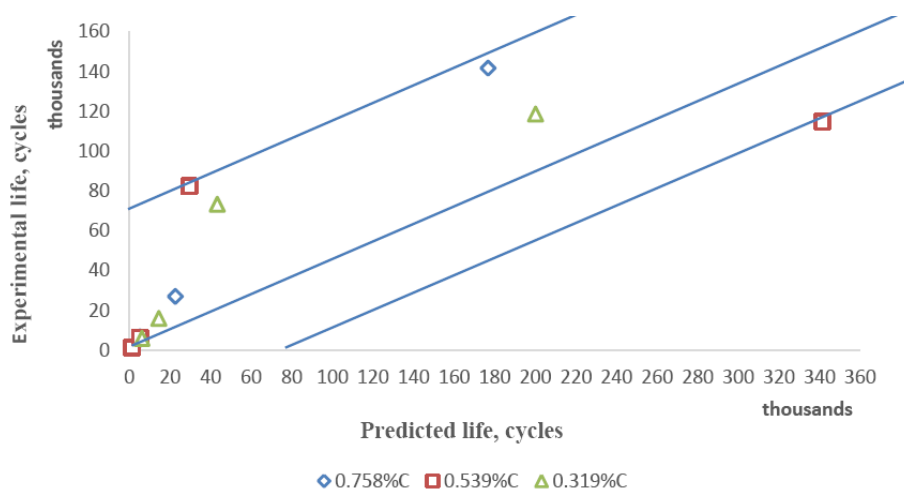


Figure 9. Comparison between predicted life and experimental one at 100°C.

## 7. Conclusions

Based on the analysis of the experimental results, some remarks can be derived:

- 1- The fatigue life and strength significantly reduced at elevated temperature (100°C) compared to the room temperature.
- 2- The fatigue strength of 0.539%C content revealed high resistance to cyclic loading and showing less reduction in fatigue strength at 100°C environment condition i-e 15.39% compared to both alloys at 100°C testing.
- 3- The fatigue life of 0.539%C gave higher experimental and predicted fatigue life at 100°C compared with the other two alloys close to the fatigue limit.
- 4- The predicted life to experimental life ratio was obtained around unity i-e within the fatigue scatter for the three alloys used.
- 5- Increasing carbon content percentage improved the fatigue strength and life up to 0.539%C and after that the fatigue strength and life became slightly reduced.

## References

- [1] Gandy D. Carbon steel handbook. Electric Power Research Institute Inc, 2007.
- [2] Thabat M.A. Aboud. Effect of carbon content percentage of steel alloys on cumulative hot creep-fatigue interaction. MS.c. Thesis, University of AL-Mustansiriya, College of Engineering, Materials Engineering Department, 2012.
- [3] Deiter G.E. Mechanical metallurgy. McGraw-Hill Book Company, pp.375, 378,379, 1988.
- [4] American society for metals. Metals handbook. Metals park, Ohio, vol.10, 1975.
- [5] Christ H.J., Jung A., Maier H.J., Teteruk R. Thermo-mechanical fatigue damage mechanisms and mechanism-based fatigue life prediction methods. Sadhana, vol 28, pp.147-165., 2003.
- [6] Milne I., Ritchie R.O., Karihaloo B. Comprehensive Structural Integrity. Elsevier Science, vol 5.03, P115, 2003.
- [7] Parka J.I., Kimb C.K., Leeb S. Evaluation of thermal fatigue properties of HSS roll materials. Hradec nad Moravicí, 2003.
- [8] Agbadual S.A., Mgbemenal C.O., Mgbemena C.E., Chima L.O. Thermal cycling effects on the fatigue behaviour of low carbon steel. Journal of Minerals & Materials Characterization & Engineering, vol. 10, No.14, pp.1345-1357, 2011.
- [9] Bader Q., Kadum E. Mean stress correction effects on the fatigue life behavior of steel alloys by using stress life approach theories. International Journal of Engineering & Technology IJET-IJENS, vol 10, p50, 2014.
- [10] Gallo P., Berto F. High temperature fatigue tests and crack growth in 40CrMoV13.9 notched components. Frattura e Integrita Strutturale, vol 34, p180, 2015.
- [11] Standard specification for steel bars, carbon and alloy, hot wrought, general requirements, Designation: ASTM A29/A 29M-05 EDT, 2006.
- [12] Samborsky D.D. Fatigue of E-glass fiber reinforced composite material and substructures. M.Sc. Thesis, Montana State University Internal Report, Civil Engineering Department, 1999.
- [13] Mustafa B.H. Al-khafaji. Experimental and theoretical study of composite material under static and dynamic loadings with different temperature conditions. Ph.D. Thesis, University of technology, 2014.
- [14] H.J.Mohamed Alalkawi, Thabat.M.Ali, Abdul Muhssan, kiffaya Al-Saffar. Influence of Carbon Content on elevated temperature fatigue properties of different steel alloys. Eng. & Tech. Journal, vol.30, No.8, 2012.
- [15] H.J.Mohamed Alalkawi, Thabat.M.Ali, kiffaya Al-saffar. Life prediction model for cumulative fatigue – creep interaction, to be published, 2012.